

Salt Partitioning in Cationic Thermoresponsive Hydrogels for Model-Seawater Desalination


Amir Jangizehi and Sebastian Seiffert*

Charged hydrogels partially reject salt ions during swelling in a salt solution reservoir. This feature suggests applicability for the separation of salt ions from saline water for water desalination in a membrane-free forward osmosis process. In this work, model charged cationic and thermoresponsive hydrogels are prepared and their potential for desalination of model seawater containing both monovalent and divalent ions with concentrations of 0.11–3.5 wt% is investigated. The recovery of adsorbed water, after partial salt rejection, is achieved by heating the hydrogels. The salt rejection increases upon increase of the charge density of the hydrogels and diminishes by increase of the concentration of the salt solution. In addition, the salt rejection during deswelling of the hydrogels is in the opposite of the overall process target, adding another challenge on the efficiency of the approach. Besides the experimental results, equations based on the Donnan theory are derived to predict the salt rejection of hydrogels during swelling and deswelling processes. While the theoretical values deviate from the experimental ones, the theory predict the overall trend well. Both experimental and theoretical results confirm that this approach has considerable potential for the desalination of saline water at low concentrations such as brackish waters.

1. Introduction

Hydrogels have many applications in our daily life, like packaging of food, medicine, or in the form of hygiene and cosmetic products.^[1] Among different types of hydrogels, charged hydrogels have a specific property, which is the ability of water adsorption in a range of 10–1000 times of their own dry weight.^[2] In addition to different applications of such materials due to the high water adsorption capacity, such as in diapers, the potential of using charged hydrogels as draw agents in forward osmosis desalination has been recently introduced and investigated.^[3–8]

A. Jangizehi, S. Seiffert
 Department of Chemistry
 Johannes Gutenberg University of Mainz
 Duesbergweg 10-14, D-55128 Mainz, Germany
 E-mail: sebastian.seiffert@uni-mainz.de

 The ORCID identification number(s) for the author(s) of this article can be found under <https://doi.org/10.1002/macp.202200070>

© 2022 The Authors. Macromolecular Chemistry and Physics published by Wiley-VCH GmbH. This is an open access article under the terms of the Creative Commons Attribution License, which permits use, distribution and reproduction in any medium, provided the original work is properly cited.

DOI: 10.1002/macp.202200070

The physical origin behind this feature is explained by the Flory–Rehner theory, in which the adsorption of water by hydrogels during swelling is considered as osmosis driven by the difference of the osmotic pressure between the gel and water.^[9,10] In this theory, the osmotic pressure of hydrogels is defined by the summation of enthalpic, entropic, and ionic terms. The first two terms are in common with non-charged hydrogels. The ionic term, π_{ion} , is specific for the charged hydrogels and is expressed as $\pi_{\text{ion}} = RT \sum [(C_j)^{\text{gel}} - (C_j)^{\text{s}}]$, where $(C_j)^{\text{gel}}$ and $(C_j)^{\text{s}}$ denote the concentration of mobile ions j inside the hydrogels and in the surrounding solution, respectively. When hydrogels swell in deionized water, $(C_j)^{\text{s}} = 0$ and $(C_j)^{\text{gel}}$ equals the concentration of the counter ions of the fixed charged groups. Therefore, for a gel with defined chemistry and crosslinking density (and thereby almost fixed enthalpic and entropic contributions), by increase of the charged groups content, and with that

increase of the concentration of $(C_j)^{\text{gel}}$, the difference of the osmotic pressure between the hydrogel and the surrounding solution increases, which leads to higher water adsorption. When charged hydrogels swell in a salt solution, $(C_j)^{\text{gel}}$ equals the summation of the concentration of the counter ions of the fixed charged groups and the mobile ions dissolved in the adsorbed solution, which generally reduces π_{ion} , and with that the hydrogel swelling capacity. Note that due to the presence of unexchangeable ionic groups in the network of gels, the concentrations of mobile ions dissolved in the adsorbed solution and in the surrounding solution are not equal. The reason for such unequal distribution of mobile ions is the constraint of charge neutrality in both phases. This phenomenon is described by the Donnan equilibrium theory, in which a so-called Donnan potential is considered for mobile ions.^[11–13] This potential is a single constant for all mobile ionic species and cancels for each neutral ionic pair. As explained in the Supporting Information, for example, if a cationic hydrogel with counter ions of Cl^- swells in an infinity NaCl solution, the Donnan equilibrium predicts that

$$(C_{\text{Na}^+})^{\text{gel}} = -\frac{(C_{\text{K}})}{2} + \sqrt{\left(\frac{C_{\text{K}}}{2}\right)^2 + [(C_{\text{Na}^+})^{\text{s}}]^2} \quad (1)$$

in which, $(C_{\text{Na}^+})^{\text{gel}}$, and $(C_{\text{Na}^+})^{\text{s}}$ are the concentration of sodium ions inside the gel and in the surrounding solution, respectively.

(C_K) is the concentration of fixed positively charged groups of the network of the hydrogel. Note that (C_{Na^+})^s equals the overall concentration of the surrounding solution, (C)^s. Equation (1) predicts that for a defined (C)^s, (C_{Na^+})^{gel} monotonically decreases by increase of (C_K). As a result, it is possible to control the level of the unequal distribution of the salt ions by the amount of the charged groups inside the network of the hydrogel (see Figure S1 in the Supporting Information). Another parameter that influences (C_{Na^+})^{gel} is (C)^s. Considering Equation (1), by increase of (C)^s, the difference of the concentration of sodium ions inside the hydrogel and in the surrounding solution gets smaller (see Figure S2 in the Supporting Information).

The salt partitioning by charged hydrogels resembles one of the main functions of semi-permeable membranes, which is the separation of ions from a salt solution reservoir.^[14–16] Combining this feature with the ability of charged hydrogels to draw water in a forward osmosis process suggests a new potential for applicability of these materials as simultaneous draw and separation agents in a so-called free-membrane forward osmosis, MFFO, desalination process.^[17,18] The lacking need for semi-permeable membranes, and the practical simplicity that comes along with that both reduce the cost of the process and can therefore be considered as potential advantages of MFFO for water desalination. This approach has been experimentally and theoretically investigated in the last decade.^[19–24] The overall process includes swelling and deswelling of hydrogels (see Scheme S1 in the Supporting Information). In the first step, charged hydrogels swell in a salt solution reservoir. The driving force of the swelling, as described by the Flory–Rehner theory, is the difference of the osmotic pressure between the hydrogels and the surrounding solution. During the water adsorption, as described by the Donnan theory, an unequal distribution of mobile ions (salt partitioning) occurs between the adsorbed and the surrounding solutions, whereby the adsorbed solution by the hydrogels has a lower concentration than the reservoir. Accordingly, this step can be considered as a forward osmosis process, in which hydrogels draw the salt solution from a reservoir and partially separate ions from it. In the second step, the swollen hydrogels are separated from the remaining (nonadsorbed) solution, and the adsorbed solution is then partially recovered (released, desorbed) through deswelling of the hydrogels.

The hydrogel deswelling can be achieved for example by application of pressure on equilibrated swollen specimen. With this approach, Wilhelm and coworkers examined the desalination of NaCl solutions with a concentration range of 1–30 g L⁻¹.^[17,19] Their results showed that the efficiency of the salt rejection depends on multiple parameters, such as the volume ratio of the salt solution and the adsorbed solution, the polymer-network crosslinking density of the hydrogels, the mole fraction of the charged groups in the polymer network, and the concentration of the salt solution. In this approach, the pressure applied to the hydrogels needs to be monotonically increased with time to get almost fixed output flux. The recovered water is commonly collected in multiple fractions. One crucial point that is observed in their results is that the concentration of the recovered water in a few of the first fractions is always higher than that of the initial solution. This observation can be understood in a sense of the Donnan theory equilibrium: during the deswelling of charged hydrogels, another unequal distribution of mobile salt ions between the hydrogels

and the desorbed solution occurs. Therefore, the concentration of the recovered water is always higher than that of the remaining solution inside the hydrogels. At the initial steps of the application of pressure, this concentration might be even higher than that of the initial solution. In the following steps and by monotonic decrease of the concentration of the remaining solution inside the hydrogels, the concentration of the recovered water decreases, and at a critical pressure, it gets smaller than the concentration of the initial salt solution.

In addition to experimental studies, the efficiency of the salt partitioning for charged hydrogels has been also theoretically investigated. Holm and coworkers simulated the compression of poly(sodium acrylate) hydrogels in multiple sequences. In each sequence, several compression steps are applied to the hydrogels, in which the pressure slowly increases up to a defined maximum value. In this simulation, each compression sequence starts after equilibrium swelling of fresh hydrogels within the recovered water of the previous sequence.^[21] The results revealed that by a single desalination sequence, the difference of the salt concentration between the desorbed water phase and the initial solution is less than 1.5%, while this difference between the remaining solution inside the hydrogels and the initial solution is up to 58%. The authors showed that by increase of the number of desalination sequences, it is possible to reach almost 100% salt partitioning for hydrogels with optimized crosslinking density and charged group content. In another work, Kosovan and coworkers investigated the compression of charged hydrogels in open and closed systems, with a target of reaching maximum thermodynamic efficiency.^[22] The results showed that the change of the ion concentration upon compression depends on the pK_a of the charged groups and the concentration of the initial salt solution. For gels with low pK_a (strong polyacids), the concentration of the recovered water is monotonically decreasing upon compression of the hydrogels. Weak polyelectrolyte gels (for example, a polyacid with pK_a = 5.6), however, may behave as weak, intermediate, or even strong polyelectrolyte gels, depending on the concentration of the initial salt solution. The authors explained this observation by considering decreasing the ionization degree upon compression of the hydrogels, and with that shifting the Donnan partitioning. Based on these findings, the authors proposed a fully reversible desalination cycle by using a low concentration and a high concentration salt solution reservoir and shifting the swelling and deswelling steps in open and closed systems. In two more recent works, Kosovan and coworkers investigated the influence of the charge–charge interactions and the concentration of the initial salt solution on the ionization degree of weak polyacids, considering the Donnan effect, since variation of the ionization degree potentially affects the swelling and the salt partitioning features of the hydrogels.^[23,25]

In addition to applying pressure on hydrogels, other types of stimuli like heating or magnetic field can also be considered to induce hydrogel deswelling.^[7,26] By using thermoresponsive hydrogels, for example, several advantages might be added to the process such as the recovery of the adsorbed water by heating the hydrogels with low-price heat sources, which potentially reduces the process cost. In this sense, charged, thermoresponsive hydrogels formed from *N*-isopropyl acrylamide, NiPAAm, and sodium acrylate, SA, have been investigated in MFFO processes. For these hydrogels, the salt rejection efficiency depends

on the molecular architecture of the polymer network. For a defined content of the charged groups, comb-like copolymer hydrogels revealed significantly higher salt rejection than copolymers with random copolymer architecture.^[26,27] Recently, we systematically studied a library of charged, thermoresponsive hydrogels formed by chemically crosslinked random copolymers of NiPPAm and SA with different charged groups contents and crosslinking densities.^[28] The experimental results as well as the Donnan theory demonstrated that the volume ratio of the recovered water to the adsorbed solution has a direct influence on the overall salt rejection efficiency of the process. Accordingly, the report of Gutmann and coworkers on the influence of the polymer-network molecular architecture on the salt rejection efficiency was attributed to the improvement of the water recovery by changing the microstructure from the random copolymer to the comb-like architecture.^[26,27] In addition, in our previous study, almost negative quantities for the salt rejection efficiency were reported, which was the consequence of undesired salt partitioning in the water recovery step as well as collecting the recovered water in one fraction. By following the experiment with a second step of the hydrogel shrinking or by gradually increase of the temperature and collecting the recovered water in multiple fractions, it was possible to significantly improve the salt rejection efficiency even by using hydrogels with relatively low amount of the charged groups.

While the results of the mentioned studies on the utility of charged, thermoresponsive hydrogels in MFFO process give a general view on the potential and challenges of this approach for the desalination of saline water, there are still some important aspects that need to be further studied. One of these aspects is the effect of the charged groups on the deswelling ability of hydrogels, which is one of the main challenges that the MFFO approach and membrane-based FO process have in common: the volume phase transition temperature, VPTT, of NiPAAm-SA random copolymer hydrogels increases by increase of the sodium acrylate content, such that hydrogels with 10 mol% of SA do not show a transition point below 60 °C.^[28] Another aspect is the effect of multivalent ions on the overall efficiency of the MFFO process. In most of the previous studies, NaCl solution was selected as a model of saline water. However, in real applications, the presence of multivalent ions like Mg²⁺ or Ca²⁺, which may form additional physical crosslinks in the network of hydrogels if that contains carboxy groups or the like, should also be considered. To investigate this effect, the performance of model cationic hydrogels for desalination of seawater with MFFO process has been recently investigated.^[20] The results demonstrated that the swelling capacity of these hydrogels in model seawater is almost identical to that of anionic hydrogels with similar ionic strength in sodium chloride solutions. With optimized hydrogel parameters, a salt rejection of 40% from model seawater with a concentration of 11.6 g L⁻¹ was achieved. However, obtaining this considerable capacity may face several challenges if the cationic hydrogels are thermoresponsive as well and the shrinking step is done in one-step as observed before for the salt rejection of anionic hydrogels in NaCl solution.

In this work, these challenges are investigated with the study of the salt partitioning to investigate the potential as well as the challenges of water desalination by cationic, thermoresponsive hydrogels. We use a library of hydrogels based on random copoly-

mers of NiPAAm and (3-Acrylamidopropyl)trimethylammonium chloride, AAPTMA, and we investigate their performance as a simultaneous draw and separation agent in MFFO process to desalinate model seawaters with different concentrations. In addition to these experiments, equations based on the Donnan theory are derived to predict the concentration of the supernatant phase and the recovered water, and to compare the theoretical results with the experimental data. The results show a significant potential of MFFO method for desalination of brackish water.

2. Model

2.1. Donnan Equilibrium for the Swelling of Cationic Hydrogels in Model Seawater Containing Divalent Ions

When cationic hydrogels are placed in seawater, they start to take up the salt solution until reaching their swelling equilibrium. At this state, the chemical potentials of each ionic component in the hydrogels, $\mu(j)^{\text{gel}}$, and in the supernatant phase, $\mu(j)^{\text{sup}}$, are equal

$$\mu(j)^{\text{gel}} = \mu(j)^{\text{sup}} \quad (2)$$

where

$$\mu(j)^{\text{gel}} = \mu(j)^{\text{ref}} + \mu(j)^{\text{id,gel}} + \mu(j)^{\text{ex,gel}} + v_j \mu^{\text{Don}} \quad (3)$$

$$\mu(j)^{\text{sup}} = \mu(j)^{\text{ref}} + \mu(j)^{\text{id,sup}} + \mu(j)^{\text{ex,sup}} \quad (4)$$

$\mu(j)^{\text{ref}}$, $\mu(j)^{\text{id}}$, $\mu(j)^{\text{ex}}$, denote the reference, ideal, and excess chemical potential, respectively, in the corresponding phase (gel: the adsorbed solution inside the gel; sup: the supernatant phase). v_j , and μ^{Don} are the valency of the ion and the Donnan potential, respectively. The latter term in Equation (3) should be considered in the expression of the chemical potential due to the unequal distribution of the mobile ions between the hydrogels and the supernatant phase. This potential is a single constant for all exchangeable ions. By ignoring the excess chemical potential, we get

$$\mu(j)^{\text{id,gel}} - \mu(j)^{\text{id,sup}} = -v_j \mu^{\text{Don}} \quad (5)$$

Considering the definition of the ideal chemical potential, Equation (5) can be written based on the concentration of the ionic species j in the hydrogels, $(C_j)^{\text{gel}}$, and in the supernatant phase, $(C_j)^{\text{sup}}$

$$k_B T [\ln(C_j)^{\text{gel}} - \ln(C_j)^{\text{sup}}] = -v_j \mu^{\text{Don}} \quad (6)$$

$$\frac{(C_j)^{\text{gel}}}{(C_j)^{\text{sup}}} = \exp\left(\frac{-v_j \mu^{\text{Don}}}{k_B T}\right) \quad (7)$$

or

$$\left[\frac{(C_j)^{\text{gel}}}{(C_j)^{\text{sup}}}\right]^{1/v_j} = \exp\left(\frac{-\mu^{\text{Don}}}{k_B T}\right) \quad (8)$$

Since the Donnan potential is a single constant for all exchangeable ionic species, it is possible to establish a relationship between the concentration ratio of ionic species in the hydrogels and in the supernatant phase. In studied model seawater in this work, for example

$$\left[\frac{(C_{\text{Na}^+})^{\text{gel}}}{(C_{\text{Na}^+})^{\text{sup}}} \right]^2 = \left[\frac{(C_{\text{Mg}^{2+}})^{\text{gel}}}{(C_{\text{Mg}^{2+}})^{\text{sup}}} \right] = \left[\frac{(C_{\text{Ca}^{2+}})^{\text{gel}}}{(C_{\text{Ca}^{2+}})^{\text{sup}}} \right]$$

$$= \left[\frac{(C_{\text{Cl}^-})^{\text{sup}}}{(C_{\text{Cl}^-})^{\text{gel}}} \right]^2 = \left[\frac{(C_{\text{SO}_4^{2-}})^{\text{sup}}}{(C_{\text{SO}_4^{2-}})^{\text{gel}}} \right] \quad (9)$$

In addition, for each mobile ion, a mass balance during the swelling step must be considered

$$(C_j)^s V_s = (C_j)^{\text{gel}} V_{\text{gel}} + (C_j)^{\text{sup}} V_{\text{sup}} \quad (10)$$

where V_s , V_{gel} , and V_{sup} denote the volumes of the initial salt solution, hydrogel, and supernatant phase, respectively.

Considering the experimental design in this work, we have

$$V_s = 2V_{\text{gel}} = 2V_{\text{sup}} \quad (11)$$

and therefore

$$(C_j)^{\text{gel}} = 2(C_j)^s - (C_j)^{\text{sup}} \quad (12)$$

or

$$\left[\frac{(C_j)^{\text{gel}}}{(C_j)^{\text{sup}}} \right] = \left[\frac{2(C_j)^s}{(C_j)^{\text{sup}}} \right] - 1 \quad (13)$$

For the mass balance of chloride ions, the concentration of the counterions inside the network of the hydrogels before starting the swelling process, (C_K) , should be also considered. Therefore

$$\left[\frac{(C_{\text{Cl}^-})^{\text{gel}}}{(C_{\text{Cl}^-})^{\text{sup}}} \right] = \left[\frac{2(C_{\text{Cl}^-})^s + C_K}{(C_{\text{Cl}^-})^{\text{sup}}} \right] - 1 \quad (14)$$

With Equations (13) and (14), it is possible to determine the concentration of mobile ions inside the hydrogels as a function of their concentrations in the supernatant phase, the initial salt solution, and the concentration of the fixed-charge groups. To have only one unknown variable, Equations (13) and (14), expression (9), and the condition of charge neutrality in the supernatant phase, should be simultaneously considered. This approach is described in the following:

The charge neutrality in the supernatant phase is expressed as

$$(C_{\text{Na}^+})^{\text{sup}} + 2(C_{\text{Mg}^{2+}})^{\text{sup}} + 2(C_{\text{Ca}^{2+}})^{\text{sup}} = (C_{\text{Cl}^-})^{\text{sup}} + 2(C_{\text{SO}_4^{2-}})^{\text{sup}} \quad (15)$$

Equation (13) for sodium ions is re-expressed by defining a new parameter, α

$$\left[\frac{(C_{\text{Na}^+})^{\text{gel}}}{(C_{\text{Na}^+})^{\text{sup}}} \right] = \left[\frac{2(C_{\text{Na}^+})^s}{(C_{\text{Na}^+})^{\text{sup}}} \right] - 1 = \alpha - 1 \quad (16)$$

$$(C_{\text{Na}^+})^{\text{sup}} = \frac{2(C_{\text{Na}^+})^s}{\alpha} \quad (17)$$

For magnesium ions, Equation (13) is expressed as

$$\left[\frac{(C_{\text{Mg}^{2+}})^{\text{gel}}}{(C_{\text{Mg}^{2+}})^{\text{sup}}} \right] = \left[\frac{2(C_{\text{Mg}^{2+}})^s}{(C_{\text{Mg}^{2+}})^{\text{sup}}} \right] - 1 \quad (18)$$

By considering the relationship between the concentration of magnesium ions and sodium ions introduced in expression (9), the concentration ratio of magnesium ions in the gel and the supernatant phase can be redefined by parameter α

$$\left[\frac{(C_{\text{Mg}^{2+}})^{\text{gel}}}{(C_{\text{Mg}^{2+}})^{\text{sup}}} \right] = \left[\frac{(C_{\text{Na}^+})^{\text{gel}}}{(C_{\text{Na}^+})^{\text{sup}}} \right]^2 = (\alpha - 1)^2 \quad (19)$$

Combining Equations (18) and (19) yields

$$\left[\frac{2(C_{\text{Mg}^{2+}})^s}{(C_{\text{Mg}^{2+}})^{\text{sup}}} \right] - 1 = (\alpha - 1)^2 \quad (20)$$

or

$$(C_{\text{Mg}^{2+}})^{\text{sup}} = \left[\frac{2(C_{\text{Mg}^{2+}})^s}{(\alpha - 1)^2 + 1} \right] \quad (21)$$

Similarly, for the other ions, it is possible to determine the corresponding concentration in the supernatant phase as a function of the ion concentration in the initial salt solution and parameter α

$$(C_{\text{Ca}^{2+}})^{\text{sup}} = \left[\frac{2(C_{\text{Ca}^{2+}})^s}{(\alpha - 1)^2 + 1} \right] \quad (22)$$

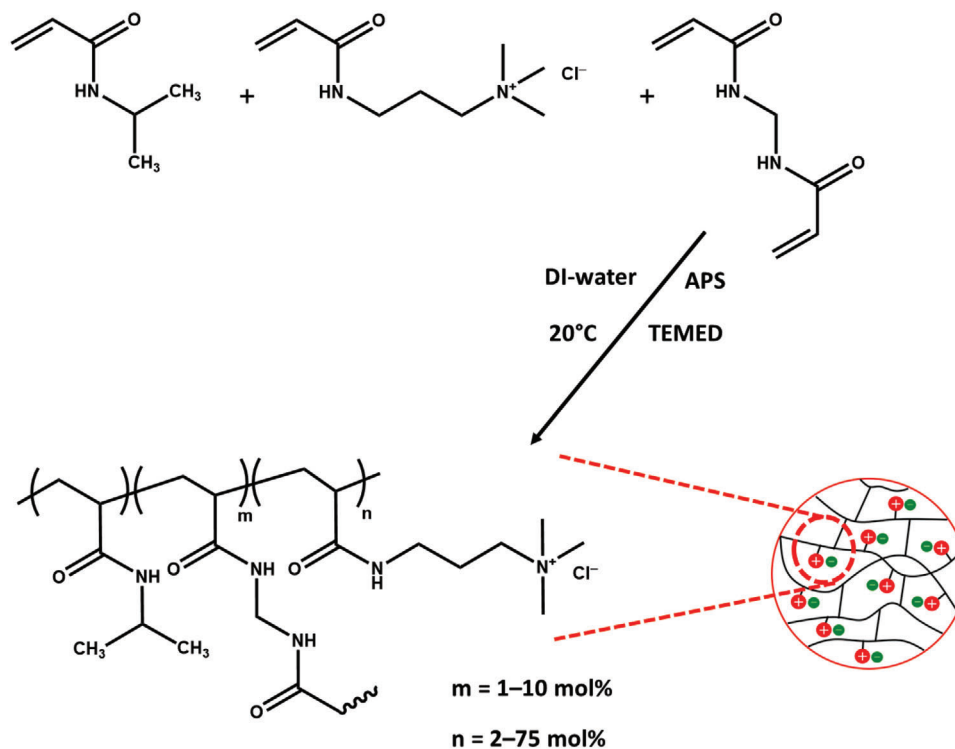
$$(C_{\text{SO}_4^{2-}})^{\text{sup}} = \left[\frac{2(C_{\text{SO}_4^{2-}})^s \times (\alpha - 1)^2}{(\alpha - 1)^2 + 1} \right] \quad (23)$$

$$(C_{\text{Cl}^-})^{\text{sup}} = \left[\frac{2(C_{\text{Cl}^-})^s + C_K \times (\alpha - 1)}{(\alpha - 1) + 1} \right] \quad (24)$$

Replacing Equations (17) and (21–24) in Equation (15) results in an equation in which parameter α is the only unknown variable

$$\frac{2(C_{\text{Na}^+})^s}{\alpha} + 2 \left[\frac{2(C_{\text{Mg}^{2+}})^s}{(\alpha - 1)^2 + 1} \right] + 2 \left[\frac{2(C_{\text{Ca}^{2+}})^s}{(\alpha - 1)^2 + 1} \right]$$

$$= 2 \left[\frac{2(C_{\text{SO}_4^{2-}})^s \times (\alpha - 1)^2}{(\alpha - 1)^2 + 1} \right] + \left[\frac{2(C_{\text{Cl}^-})^s + C_K \times (\alpha - 1)}{(\alpha - 1) + 1} \right] \quad (25)$$



Scheme 1. Synthesis of hydrogels based on *N*-isopropylacrylamide (NiPAAm) and (3-Acrylamidopropyl)trimethylammonium chloride (AAPtMA), which are crosslinked by *N,N'*-methylenebisacrylamide (MBA). The hydrogels are synthesized by free radical copolymerization at room temperature by using ammonium persulfate (APS) as initiator and the tetramethylethylenediamine (TEMED) as accelerator for radical formation. The synthesized samples have a 3D network structure.

Equation (25) can be numerically solved to determine parameter α . By determining this parameter, the concentration of all ionic species in the supernatant phase can be calculated considering Equations (17) and (21–24). In addition, the concentration of these ionic species inside the hydrogel phase can be estimated by considering the determined concentrations in the supernatant phase and Equations (13) and (14).

3. Results and Discussion

3.1. Swelling and Deswelling of Hydrogels; VPTT of Hydrogels

The hydrogels studied in this work are random copolymers of *N*-isopropylacrylamide (NiPAAm) and (3-Acrylamidopropyl)trimethylammonium chloride (AAPtMA), which are crosslinked by *N,N'*-methylenebisacrylamide (MBA). The hydrogels are synthesized by free radical crosslinking copolymerization at 20 °C, as presented in **Scheme 1**. The amount of comonomers is between 2 and 10 mol%, and the degree of crosslinking, DC, is varied between 1 and 10 mol%. For DC = 5 and 10 mol%, samples with 75 mol% of AAPtMA are synthesized as well to check the effect of high charged group content on the studied properties. The molecular and material characteristics of the synthesized hydrogels are summarized in Table S1 in the Supporting Information.

The swelling equilibrium of these hydrogels is studied in DI-water and in model seawaters with concentrations of 1.15, 2.30, 11.54, and 34.90 g L⁻¹. The quantities of the swelling capacity are

shown in **Figure 1**. For a defined DC and salt concentration, the swelling capacity increases upon increase of the comonomer content, which can be assigned to the increase of the osmotic pressure of the hydrogels due to the increase of π_{ion} . Moreover, Q_{eq} decreases by increase of the salt concentration. This reduction is related to the lower difference of $(C_j)^{\text{gel}}$ and $(C_j)^{\text{sup}}$ for a solution with a higher salt concentration. For all DC, the reduction of the swelling capacity is relatively sharp by increase of the salt concentration up to $C_s = 2.34 \text{ g L}^{-1}$, which then gets shallower for higher salt concentration. Such a nonlinear dependence is explained by considering Equation (7), where demonstrates that $(C_j)^{\text{gel}}$ and $(C_j)^{\text{sup}}$ ($(C_j)^s$ in infinity salt bath) has an exponential relationship. In addition, Q_{eq} of all samples in model seawater and NaCl solution with identical concentrations are compared in **Figure 1**. The results reveal that the presence of divalent ions in the salt solution has a low impact on the swelling capacity of our studied cationic hydrogels. This almost negligible effect is even observed for samples with 75 mol% of charged groups. In contrast to this observation, investigation of the anionic hydrogels based on NiPAAm and SA in NaCl solution and model seawater demonstrates that the difference of the Q_{eq} is significant for samples with such high content of the charged groups (see **Figure S3** in the Supporting Information). This difference is probably due to the additional physical crosslinks that can be formed between the negatively charged acrylate groups and the divalent cations.

The volume phase transition of the hydrogels is investigated in 1.15 g L⁻¹ model seawater. The results of samples with DC = 1 mol% are shown in **Figure 2A**. The data of other samples

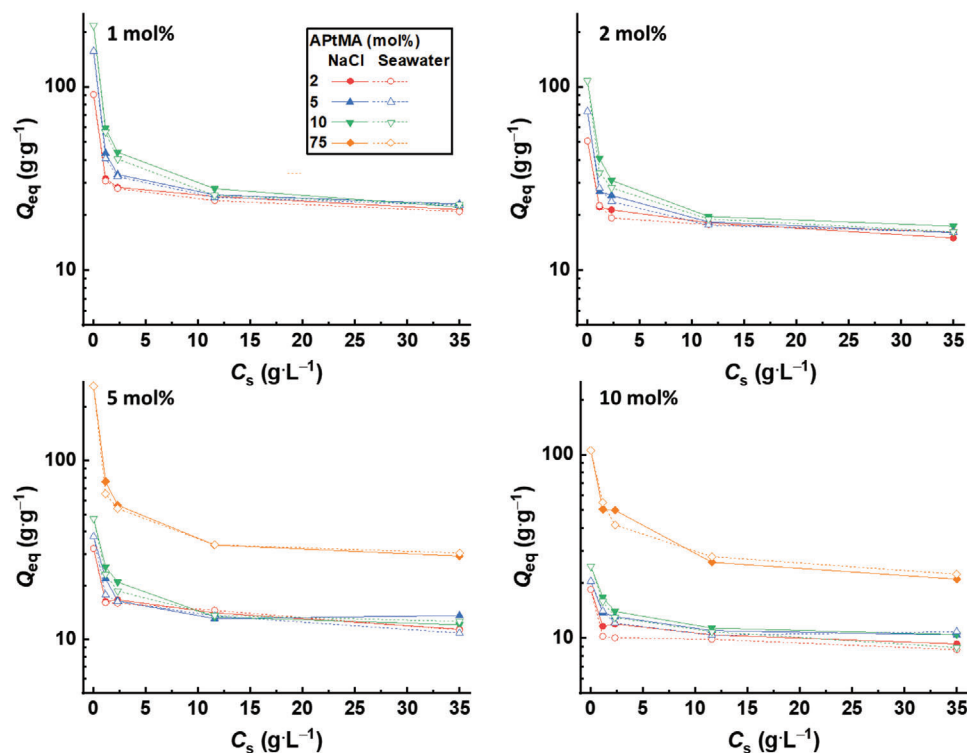


Figure 1. Equilibrium swelling of the studied cationic hydrogels in NaCl solution and model seawater as a function of the charged group content, degree of crosslinking, and the concentration of the salt solution reservoir.

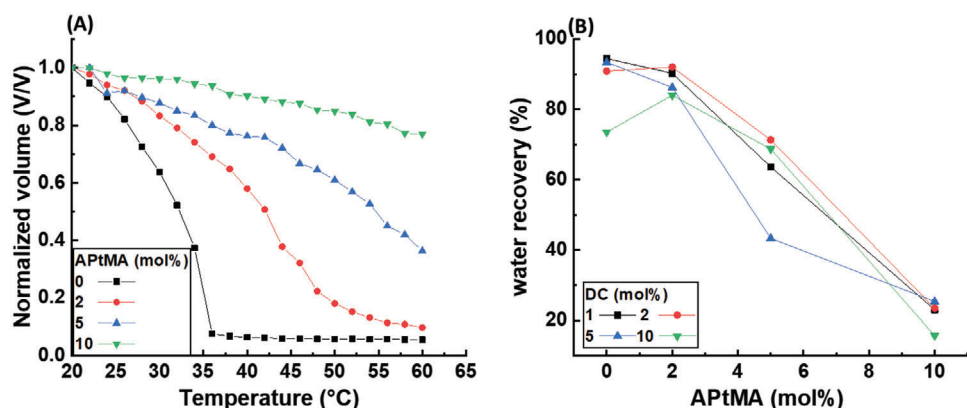


Figure 2. A) Normalized volume of the studied hydrogels with DC = 1 mol% as a function of temperature. The normalized volume is defined as the ratio of the hydrogel volume at a specific temperature to that at 25 °C. B) Water recovery of the studied hydrogels as a function of the charged group content and the crosslinking density.

is presented in Figure S4 in the Supporting Information. The hydrogels with no charged groups show discontinuous volume phase transitions. The transition gets almost continuous by addition of 2 mol% of the charged comonomers into the network of the hydrogels. In addition, the transition looks more continuous upon increase of the crosslinking density. For each sample with 0 or 2 mol% of charged groups, a distinct temperature can be assigned to the transition considering the quantities of $\Delta V/\Delta T$. For samples with 5 mol% of the charged comonomers, a distinct VPT can be determined only for the hydrogels with 1 or 2 mol% of the

crosslinking density. By increase of DC to 10 mol%, no distinct transition can be assigned for all samples. Instead, a continuous, shallow decrease of the volume is observed upon increase of temperature. Another important parameter in a sense of the hydrogel shrinking is the deswelling ability, which can be defined as the volume ratio of the deswollen gel at the final temperature and the swollen gel at 20 °C. Note that this ratio equals $1 - r_w$, where r_w is the water recovery, which is defined in Equation (29). Variation of r_w upon change of the hydrogel parameters is presented in Figure 2B, which reveals that the influence of the charged group

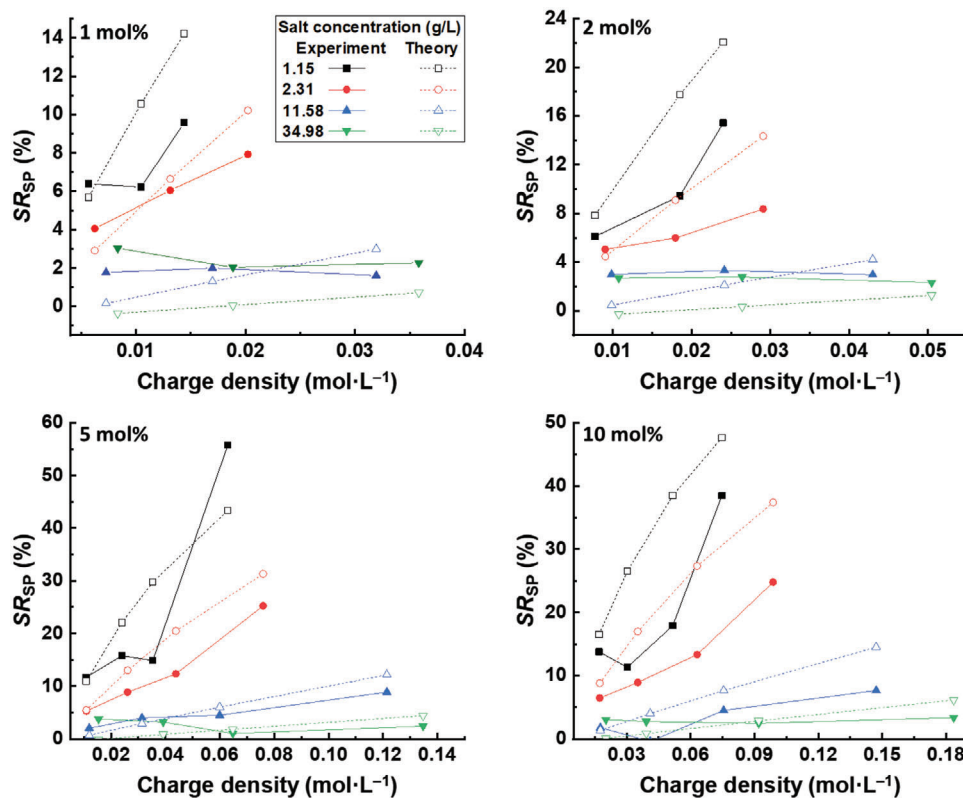


Figure 3. Salt rejection in the supernatant phase in the desalination experiment as a function of the charge density, crosslinking density (upper left numbers), and the concentration of the initial salt solution.

content on the water recovery is much stronger than that of the crosslinking density. The volume phase transition of the hydrogels also depends on the concentration of the adsorbed solution. To investigate this parameter, samples NiPAA2_2_10 swollen in model seawaters with different concentrations are heated under an optical microscope. The results are presented in Figure S5 in the Supporting Information. Upon increase of the salt concentration in the adsorbed solution, the transition gets more discontinuous and the VPTT of the hydrogels significantly decreases. The VPTT of NiPAA2_2_10 swollen in 34.9 g L⁻¹ model seawater, for example, is almost identical to the VPTT of the corresponding sample with no ionic groups swollen in 1.15 g L⁻¹ model seawater. However, the concentration of the adsorbed solution has a negligible effect on the overall deswelling ability, such that the normalized volumes of all samples at 60 °C are almost identical.

3.2. Salt Rejection Efficiency

In the first step of the desalination experiment, the hydrogels are swollen overnight in model seawaters with different concentrations. The amount of the salt solution utilized in this experiment is two times Q_{eq} calculated from the equilibrium swelling measurements. From a practical viewpoint, the experiment should be done in an infinite salt bath starting with the partially swollen hydrogels containing a volume of the adsorbed solution that equals the volume of the remained solution in the second step of the experiment. However, to make a systematic comparison between

the results of this work and those of the previous studies on model anionic hydrogels, the experiments are run in a finite salt bath starting from the dried gels.

After separation of the equilibrated swollen hydrogels from the nonadsorbed solution (supernatant phase), the concentration of the supernatant phase is estimated by measurement of its conductivity. The salt rejection, SR , in the supernatant phase is defined as

$$SR_{sup} = \frac{(C)^{sup} - (C)^s}{(C)^s} \quad (26)$$

The quantities of the salt rejection in model seawaters with different concentrations are shown in **Figure 3**. Generally, the salt rejection increases by increase of the charge density. This dependency as well as the individual quantities of the salt rejection gets shallower and smaller by increase of the salt concentration, such that at the upper extreme of the studied concentration in this work, 34.9 g L⁻¹, the salt rejection is almost negligible. This low efficiency cannot be improved for example by increase of the charge density through addition of the comonomer content even up to 75 mol%. Moreover, for samples with almost identical charged group content, the salt partitioning in brackish water can be improved by increase of the crosslinking density. This observation is related to the increase of the charge density due to the reduction of the swelling ability. This effect is however very weak for salt partitioning in high concentration model seawaters. To understand the effect of different parameters on the salt rejection

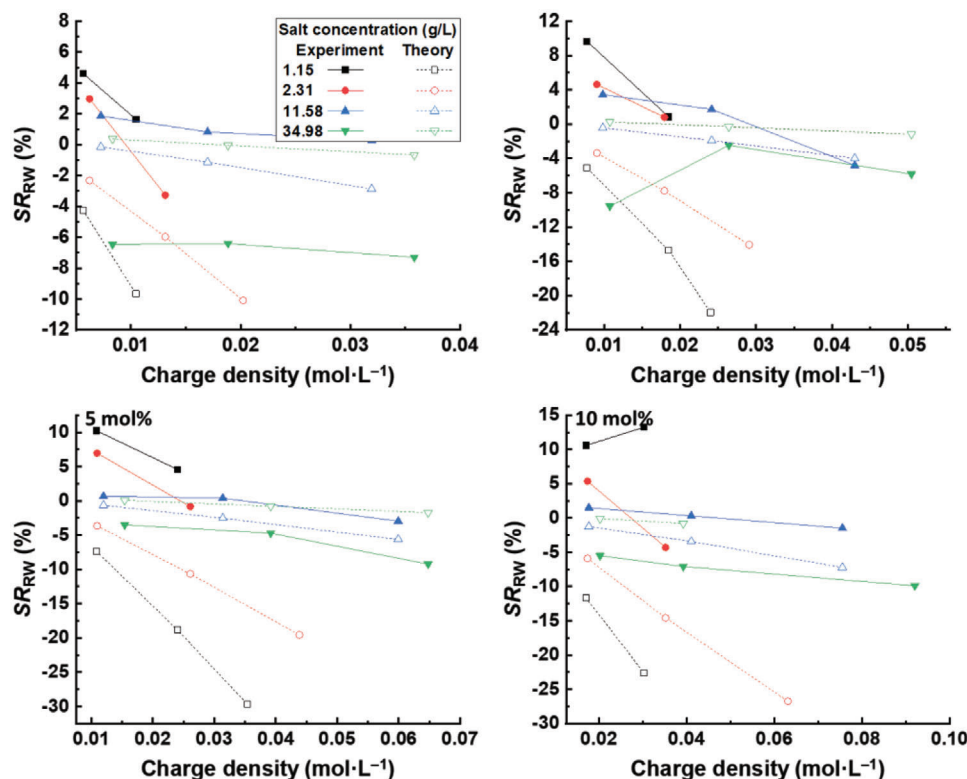


Figure 4. Salt rejection of the recovered water in the desalination experiment as a function of the charge density, crosslinking density (upper left numbers) and the concentration of the initial salt solution.

efficiency, the salt partitioning can be analyzed with the Donnan theory, as explained in Model. By solving Equation (25) for each sample, the concentration of all ions in the supernatant phase can be determined. With that, an overall concentration with the dimension of g L^{-1} is obtained, which can be then compared with the corresponding experimental quantity. The results are shown in Figure 3. The Donnan theory relatively predicts the overall trend of the change of the salt rejection as a function of the charge density, crosslinking density, and the initial salt concentration. The theory, however, fails to predict the absolute values of the salt rejection, which might be related to the circumstance that in this theory, besides the charge neutrality, other effective factors such as the ion–ion interactions are not considered.

In the second step of the experiment, the swollen hydrogels are heated at 50 °C for 1 h to induce the hydrogels shrinking, followed by collecting the recovered water with a syringe. Similar to the previous step, the concentration of the recovered water is estimated by measuring its conductivity. The salt rejection of the recovered water is defined as

$$SR_r = \frac{(C)^s - (C)^r}{(C)^s} \quad (27)$$

where $(C)^r$ is the concentration of the recovered water phase. The data of the salt rejection in this phase is presented in **Figure 4**. In opposite to the supernatant phase, the salt rejection generally decreases by increase of the charge density. The reason for this observation can be explained by considering that the

salt partitioning occurs in the deswelling process as well. Considering the fixed charged groups inside the network of the hydrogels, the overall concentration of the remained solution inside the deswollen hydrogels is always lower than that of the desorbed solution. Depending on the level of the salt partitioning in this step, the concentration of the recovered water can be lower, almost equal, or even higher than the concentration of the initial salt solution, which results in a positive, almost zero, or even negative salt rejection, respectively.

Again, it is possible to estimate the concentration of the recovered water, and with that the salt rejection, based on the Donnan theory. As explained in the Supporting Information, by considering the Donnan potential as a single constant for all mobile ionic species, the charge neutrality in the recovered water phase can be written as

$$\frac{(C_{\text{Na}^+})^{\text{gel}}}{\beta(1-r_w) + 2r_w - 1} + 2 \frac{(C_{\text{Mg}^{2+}})^{\text{gel}}}{(1-r_w)(\beta-1)^2 + r_w} + 2 \frac{(C_{\text{Ca}^{2+}})^{\text{gel}}}{(1-r_w)(\beta-1)^2 + r_w} = 2 \frac{(C_{\text{SO}_4^{2-}})^{\text{gel}}}{\frac{(1-r_w)}{(\beta-1)^2} + r_w} + \frac{(C_{\text{Cl}^-})^{\text{gel}}}{\frac{(1-r_w)}{(\beta-1)} + r_w} \quad (28)$$

where, r_w is the water recovery and is defined as

$$r_w = 1 - \frac{V_{\text{dsg}}}{V_{\text{gel}}} \quad (29)$$

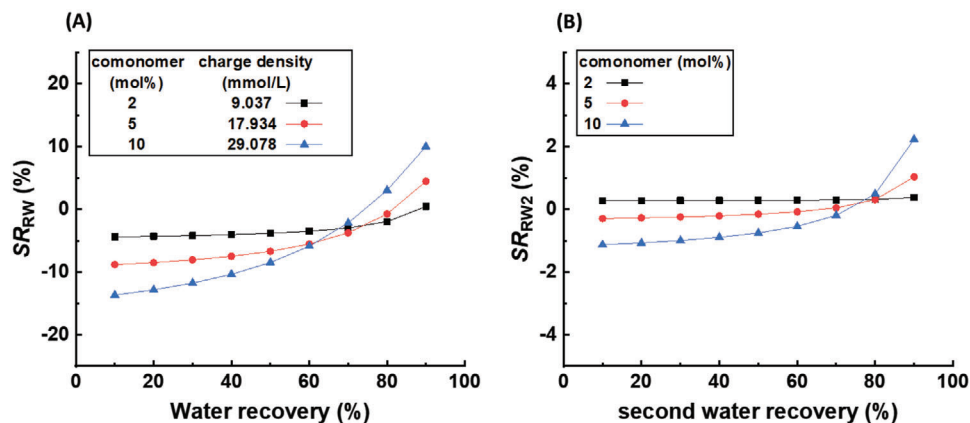


Figure 5. Salt rejection efficiency as a function of the water recovery in A) the first step and B) in the second step of the water recovery. The experiment starts with the swelling of hydrogels with DC = 2 mol% in model seawater with a concentration of 2.34 g L⁻¹.

V_{dsg} and V_{gel} are the volumes of the deswollen and swollen gel, respectively. For each sample, Equation (28) is numerically solved to derive parameter β . With this parameter, the concentration of all mobile ionic species, and with that the overall concentration of the recovered water, can be calculated as explained in the Supporting Information. The quantities of the salt rejection determined by this approach are presented in Figure 4. There is a considerable difference between the experimental and theoretical data, which is even stronger than that observed for the supernatant phase in Figure 3. In addition to ignoring the effective factors like ion–ion interactions, another reason for this relatively strong deviation is the quantities of $(C_i)^{\text{gel}}$ utilized in Equation (28). These values are obtained from the prediction of the Donna theory for the swelling step, which as explained before deviating themselves from the experimental quantities. Although, the theory still shows a relative success in the prediction of the overall trend of the change of the salt rejection upon variation of parameters like charge density, crosslinking density, or initial salt concentration.

In our previous work on the salt rejection of model anionic hydrogels in NaCl solution, it was shown that the final salt rejection of the recovered water phase can be significantly improved by increase of the water recovery or by change of the deswelling protocol, for example, by applying a second water recovery step to partially recover the solution that is remained inside the gel after the first shrinking step. The remained solution inside the gel has a considerably lower concentration than the initial salt solution due to the two times salt partitioning, once in the swelling step and another one in the shrinking step. Therefore, the chance that the second recovered water phase has a lower concentration than the initial salt solution is high. In this work, the potential of these approaches to increase the salt rejection efficiency is theoretically investigated for a part of the samples. Regarding the increase of the water recovery, the change of the salt rejection for samples with DC = 2 mol% in the experiments that start by swelling of the hydrogels in 2.34 g L⁻¹ model seawater is shown in Figure 5A. The predicted quantities regarding the experiments in which model seawaters with other concentrations are utilized are shown in Figure S6 in the Supporting Information. Generally, the salt rejection is improved with the increase of the water recovery, in a manner that the improvement is significantly stronger

for samples with higher content of the charged groups. At low water recovery (for example less than 50%), the salt rejection efficiencies for samples with 2 mol% of the charged groups are higher than those of the other samples. At high water recovery, however, this order might be inverse on account of the mentioned different dependency of the salt rejection on the water recovery. In addition, the increase of the salt rejection is shallower for experiments in model seawater with higher concentration such that for experiments in 34.98 g L⁻¹ model seawater, the salt rejection is almost independent on the water recovery even for the sample having the highest charged density.

The effect of the second hydrogel shrinking on the salt rejection is also investigated for sample NiPAA2_2_10 in experiments starting with 2.31 g L⁻¹ model seawater (Figure 5B) or 34.98 g L⁻¹ model seawater (Figure S7 in the Supporting Information). An improvement of the salt rejection compared to the first water recovery step is observed for samples with 5 or 10 mol% of the charged groups at the low water recovery region (for example less than 50%). Besides, comparison of the vertical axes of Figure 5A,B reveals that the increase of the water recovery is much more efficient method than conducting the second water recovery step to improve the salt rejection efficiencies.

4. Conclusion; Potentials and Challenges of MFFO Desalination

The salt rejection of charged hydrogels is a feature that might be considered for the desalination of saline waters. The presence of fixed, charged groups within the network of such hydrogels and the condition of charge neutrality enforce the concentration of the adsorbed solution to be lower than the concentration of the salt solution in the reservoir. Such unequal distribution of salt ions is described by the Donnan theory. Although, since other effective factors like ion–ion interactions are not considered in the classical Donna theory, the predicted quantities by the theory commonly deviate from the experimental data. However, the theory still shows a relative success to predict the overall trend of salt partitioning.

For designing the studied hydrogels in this work, two key features are considered: the presence of the charged groups within the network of the hydrogels and the thermoresponsivity

function. The first feature is necessary to induce the salt partitioning, and the second one provides the possibility for the hydrogel deswelling and the water recovery by variation of temperature. In addition, model seawaters containing divalent cations and anions with different concentrations covering brackish water to real seawater concentration range are utilized to study the challenges faced by this approach at real conditions. To avoid formation of physical crosslinks between the charged groups of the hydrogels and the divalent cations of the saline water, a cationic comonomer is selected to prepare the hydrogels. The salt rejection of the studied hydrogels in the supernatant phase generally increases upon increase of the charge density. The charge density individually depends on the mole percentage of the charged groups and on the polymer-network crosslinking density of the hydrogels. In addition, the salt rejection reduces by increase of the concentration of the salt solution. For high concentrated saline water, for example, 34.98 g L⁻¹ model seawater, the salt rejection is almost zero. The overall trend of these dependencies is predicted by the Donnan theory as well. One of the main challenges of MFFO approach even for the desalination of low-concentration saline water is the salt rejection during the hydrogel deswelling, which makes that the released water has a higher concentration than the remained solution inside the hydrogels. This direction of the salt rejection is opposite to the target of the process. The theory reveals that by increase of the water recovery (the amount of the water that is desorbed or released in the deswelling step), this effect can be partially compensated. However, this approach is not applicable for high concentration salt solutions, mainly due to the negligible salt rejection in the swelling step, meaning that the concentration of the adsorbed solution by the hydrogels has almost no difference from that of the initial salt solution. Our experimental observation and the theoretical prediction also explain the apparent contrary reports on the effect of the molecular architecture on salt rejection efficiency. Gutmann and coworkers reported that thermoresponsive, charged hydrogels with comb-like architecture reveal a considerable improvement in the salt rejection efficiency compared to the random copolymer hydrogels.^[27] On the other hand, Wilhelm and coworkers did not observe such improvement in experiments conducted with non-thermoresponsive, charged hydrogels with different molecular architectures.^[29] Gutmann and coworkers heated hydrogels at a fixed temperature within a defined time and then collected the released water in one fraction. As predicted by the Donnan theory, the increase of the water recovery has a direct impact on salt rejection improvement. In their works, this target was achieved by reducing the interphase of the thermoresponsive and charged parts of the hydrogels through the change of the molecular architecture. Wilhelm and coworkers, however, linearly increased the applied pressure to the hydrogels and collected the released water in multiple fractions.^[29] As explained before, the salt rejection occurs over the whole hydrogel shrinking process, such that the concentration of the released water is always higher than that of the remained solution inside the hydrogels. However, since the concentration of the remained solution monotonically decreases, the concentration of the recovered water decreases as well. Therefore, above a certain pressure, the recovered water has a lower concentration than the initial salt solution. As a consequence in this approach, at fixed charge density, the applied pressure, and the number of the collected fractions mainly control the overall salt rejection efficiency.

In summary, the experimental and theoretical results of this work confirm the potential of MFFO for desalination of brackish water containing divalent cations and anions. Considering other potential advantages of this approach, like the lack of need for semi-permeable membranes and the practical simplicity, MFFO desalination has potential to provide fresh water for settlements in dry areas that have access to brackish water resources. Nevertheless, compared to commercialized approach like reverse osmosis, the overall performance of the process is still significantly low in a sense of salt rejection and the water recovery. In addition, the approach is not applicable to concentrated saline water. The salt rejection efficiency can be improved by increase of the water recovery or by conducting a second step of the hydrogel shrinking. Yet, the first approach is more realistic regarding the low efficiency as well as the high cost of the second water recovery process. In addition, as shown elsewhere,^[28] changing the heating protocol in a manner that the collection of the recovered water in multiple fractions is possible, is another method to improve the overall performance of the process. Moreover, other experimental approaches, for example, the design of a continuous process in which swelling and shrinking of the hydrogels are shifted in open and close systems might improve the efficiency of the MFFO desalination. Investigation of these approaches in detail for desalination of brackish water is the target of our further studies.

5. Experimental Section

Materials: (3-Acrylamidopropyl)trimethylammonium chloride (AAPtMA; 75 wt% solution in water), *N*-isopropylacrylamide (NiPAAm), *N,N'*-methylenebisacrylamide (MBA), ammonium persulfate, and tetramethylethylenediamine were purchased from Sigma-Aldrich and used as received.

Hydrogel Synthesis: All hydrogels in this work were synthesized by free radical crosslinking co-polymerization. The general procedure is described elsewhere.^[28] In summary, AAPtMA was added to a solution of *N*-isopropyl acrylamide, NiPAAm, and *N,N'*-methylenebis(acrylamide), MBA, in water. The total concentration of these components is 10 wt%. The content of the positively charged comonomer was between 2 and 75 mol% and the polymer-network crosslinking density, which was defined as mol_{MBA}/(mol_{AAPtMA} + mol_{NiPAAm}) and varied between 1 and 10 mol%. Then, ammonium persulfate (0.4% of the total mole numbers of the monomers) was added to the solution. The mixture was bubbled with nitrogen for 20 min, and then tetramethylethylenediamine (10 times the amount of ammonium persulfate) was added. After 12 h, the resulting hydrogels were washed by immersing in an excess amount of deionized water for at least 72 h with changing the water each day to dissolve unreacted substances and linear chains. Hydrogels were then dried under reduced pressure in a vacuum oven. The reaction yield varied between 75% and 85%, considering the dried weight of hydrogels.

Hydrogel Equilibrium Swelling and Variation of Swelling by Temperature: The swelling of the hydrogels at equilibrium in deionized (DI) water and model seawaters with concentrations of 1.16–34.9 g L⁻¹ was measured using ≈10 mg of dried samples. The method is described elsewhere in detail.^[28] In summary, the dried hydrogels were placed on a polyamide filter paper with a mesh size of 50 μm, which was held between two metal rings. This setup was put in DI-water or model seawater solution. After 12 h, the filter paper and the swollen hydrogels were removed from the solution and weighted after gently pressing on a paper towel to remove the excess fluid. The equilibrium swelling degree, Q_{eq} , is defined as

$$Q_{eq} = \frac{m_{\text{absorbed solution}}}{m_d} = \frac{m_{\text{hydrogel}} - m_d}{m_d} \quad (30)$$

where $m_{\text{absorbed solution}}$, m_{hydrogel} , and m_{d} are the mass of the absorbed solution, the swollen hydrogels, and the dried samples, respectively. Note that in this experiment, the volume of the solution reservoir was significantly larger than that of the absorbed one. Therefore, the data obtained by this approach can be considered as the swelling capacity of the hydrogels in an infinity reservoir of DI-water or model seawater.

In addition, the shrinking properties of these hydrogels were studied by optical microscopy. The temperature increases from 20 to 60 °C at a rate of 0.2 °C min⁻¹, and a photo was taken every two minutes. These photos were analyzed by Image J software to calculate an average radius for the irregular shaped specimens. For each temperature, a volume ratio was determined by dividing the volume of the sample to the volume at 20 °C. For each sample, the corresponding volume ratio at the final temperature (60 °C) was considered as a criterion for the degree of deswelling.

Desalination Experiment: The procedure of the desalination experiment is described elsewhere.^[28] In summary, the experiment was started by swelling of dried samples in a model seawater solution with a volume of $V_s = 2 \times Q_{\text{eq}} \times m_{\text{d}}$. To determine V_s for each sample, the corresponding value of Q_{eq} determined from the equilibrium swelling experiment was utilized. Note that in this case, in opposite to the swelling of hydrogels in contact with an infinite solution, the concentration of the supernatant phase (nonabsorbed solution by hydrogels) was different from the initial salt solution due to the salt partitioning effect. According to the Flory–Rehner theory, this may change Q_{eq} . However, the accurate weighting of swollen hydrogels in the desalination experiment illustrates that the difference of Q_{eq} between these two methods was less than 5%,^[28] which was neglected in this work.

After separation of the swollen hydrogels from the supernatant phase, the hydrogels were put in a proper container, followed by putting the container in a 50 °C water bath for 1 h. The recovered (desorbed; released) water was then collected by a syringe. To estimate the concentration of the supernatant phase and the recovered water, the electric conductivity of each phase was measured (FiveEasy Plus FP30-Std-Kit conductivity meter; Mettler Toledo) and compared with calibration curves constructed by measuring the ionic conductivity of reference solutions with a concentration of 0.2–4 g L⁻¹ or 1–30 g L⁻¹.

Supporting Information

Supporting Information is available from the Wiley Online Library or from the author.

Acknowledgements

The authors gratefully thank the Federal Ministry of Science and Education of Germany (BMBF) for the financial support under project HydroDeSal (Project Code 02WME1613).

Open Access funding enabled and organized by Projekt DEAL.

Conflict of Interest

The authors declare no conflict of interest.

Data Availability Statement

The data that support the findings of this study are available from the corresponding author upon reasonable request.

Keywords

desalination, Donnan theory, forward osmosis, thermoresponsive hydrogels

Received: February 24, 2022

Revised: April 30, 2022

Published online: July 15, 2022

- [1] F. Ullah, M. B. H. Othman, F. Javed, Z. Ahmad, H. Md. Akil, *Mater. Sci. Eng.: C* **2015**, *57*, 414.
- [2] M. J. Zohuriaan Mehr, K. Kabiri, *Iran. Polym. J.* **2008**, *17*, 451.
- [3] D. Li, X. Zhang, J. Yao, Y. Zeng, G. P. Simon, H. Wang, *Soft Matter* **2011**, *7*, 10048.
- [4] D. Li, X. Zhang, J. Yao, G. P. Simon, H. Wang, *Chem. Commun.* **2011**, *47*, 1710.
- [5] D. Li, X. Zhang, G. P. Simon, H. Wang, *Water Res.* **2013**, *47*, 209.
- [6] A. Razmjou, Q. i Liu, G. P. Simon, H. Wang, *Environ. Sci. Technol.* **2013**, *47*, 13160.
- [7] A. Razmjou, M. R. Barati, G. P. Simon, K. Suzuki, H. Wang, *Environ. Sci. Technol.* **2013**, *47*, 6297.
- [8] Y. Hartanto, M. Zargar, H. Wang, B. o Jin, S. Dai, *Environ. Sci. Technol.* **2016**, *50*, 4221.
- [9] P. J. Flory, J. Rehner, *J. Chem. Phys.* **1943**, *11*, 521.
- [10] P. J. Flory, *Principles of Polymer Chemistry*, Cornell University Press, Ithaca, NY **1953**.
- [11] F. Donnan, E. Guggenheim, *Zeitschrift Physikalische Chemie* **1932**, *162*, 346.
- [12] A. Katchalsky, I. Michaeli, *J. Polym. Sci.* **1955**, *15*, 69.
- [13] P. Košován, T. Richter, C. Holm, *Macromolecules* **2015**, *48*, 7698.
- [14] H. K. Lonsdale, *J. Membr. Sci.* **1982**, *10*, 81.
- [15] Y. C. Woo, S.-H. Kim, H. K. Shon, L. D. Tijing, in *Current Trends and Future Developments on (Bio-) Membranes* (Eds: A. Basile, K. Ghasemzadeh), Elsevier, Amsterdam **2018**.
- [16] C. Tang, M. L. Bruening, *J. Polym. Sci.* **2020**, *58*, 2831.
- [17] J. Höpfner, C. Klein, M. Wilhelm, *Macromol. Rapid. Commun.* **2010**, *31*, 1337.
- [18] J. Höpfner, T. Richter, P. Košován, C. Holm, M. Wilhelm, *Hydrogels, Gels Horizons: From Science to Smart Materials*, Springer, Singapore **2013**, p. 247.
- [19] L. Arens, J. B. Albrecht, J. Höpfner, K. Schlag, A. Habicht, S. Seiffert, M. Wilhelm, *Macromol. Chem. Phys.* **2017**, *218*, 1700237.
- [20] C. Fengler, L. Arens, H. Horn, M. Wilhelm, *Macromol. Mater. Eng.* **2020**, *305*, 2000383.
- [21] T. Richter, J. Landsgesell, P. Košován, C. Holm, *Desalination* **2017**, *414*, 28.
- [22] O. Rud, O. Borisov, P. Košován, *Desalination* **2018**, *442*, 32.
- [23] O. V. Rud, J. Landsgesell, C. Holm, P. Košován, *Desalination* **2021**, *506*, 114995.
- [24] C. Yu, Y. Wang, X. Lang, S. Fan, *Environ. Sci. Technol.* **2016**, *50*, 13024.
- [25] J. Landsgesell, P. Hebbeker, O. Rud, R. Lunkad, P. Košován, C. Holm, *Macromolecules* **2020**, *53*, 3007.
- [26] W. Ali, B. Gebert, S. Altinpinar, T. Mayer-Gall, M. Ulbricht, J. Gutmann, K. Graf, *Polymers* **2018**, *10*, 567.
- [27] W. Ali, B. Gebert, T. Hennecke, K. Graf, M. Ulbricht, J. S. Gutmann, *ACS Appl. Mater. Interfaces* **2015**, *7*, 15696.
- [28] A. Jangizehi, S. Seiffert, *J. Chem. Phys.* **2021**, *154*, 144902.
- [29] L. Arens, D. Barther, J. Landsgesell, C. Holm, M. Wilhelm, *Soft Matter* **2019**, *15*, 9949.